第42卷第4期 中国科学技术大学学报 Vol. 42, No. 4
2012年4月 JOURNAL OF UNIVERSITY OF SCIENCE AND TECHNOLOGY OF CHINA Apr. 2012

Article ID: 0253-2778(2012)04-0279-10

Nonlinear flow characteristics in low-permeability reservoirs with stress sensitive effect

LIU Wenchao, YAO Jun, LI Aifen, SUN Zhixue, HUANG Zhaoqin

(*School of Petroleum Engineering, China University of Petroleum (East China), Qingdao 266555, China*)

Abstract: Based on the continuity of the derivative of the nonlinear seepage velocity function in low-permeability reservoirs, the nonlinear kinematic equation in the real number field for the low-permeability reservoirs was deduced. The mathematical formula of the apparent permeability and the apparent pseudo threshold pressure gradient were defined. It was demonstrated that the continuous derivative of the seepage velocity function was consistent with the continuous permeability change. The mathematical model of the nonlinear flow in low-permeability reservoirs with stress sensitive effect under the condition of constant well production rate was constructed. Owing to its strong nonlinearity, efficient Douglas-Jones predictor-corrector finite difference method was adopted to obtain its numerical solution. Moreover, its accuracy was verified by comparison with the numerical solution obtained by the fully implicit finite difference method. Result analysis shows: log-log curves of dimensionless transient wellbore pressure corresponding to the nonlinear kinematic equation and pseudo-linear kinematic equation both have inflexions at the initial period. And the inflexion corresponding to the pseudo-linear one is more obvious; the permeability modulus has a major effect on the second half of these curves; the bigger its value, the sharper the pressure drop; there exists a moving boundary in the nonlinear flow in low-permeability reservoirs; the moving boundary of the pseudo-linear flow moves more slowly than that of the nonlinear flow.

Key words: low-permeability reservoirs; stress sensitive effect; Douglas-Jones predictor-corrector finite difference method; nonlinear flow; moving boundary; well testing

CLC number: TE312; O357.3 **Document code**: A doi: 10.3969/j.issn.0253-2778.2012.04.004

Citation: Liu Wenchao, Yao Jun, Li Aifen, et al. Nonlinear flow characteristics in low-permeability reservoirs with stress sensitive effect[J]. Journal of University of Science and Technology of China, 2012, 42(4): 279-288.

Received: 2011-09-14; **Revised**: 2011-12-21

Foundation item: Supported by the National Key Basic Research (973) Program of China (2006CB202404).

Biography: LIU Wenchao, male, born in 1984, PhD candidate. Research field: fluid flow in porous medium and relevant application in petroleum engineering. E-mail: wcliu_2008@126.com

Corresponding author: YAO Jun, Prof. E-mail: yaojunhdpu@126.com

考虑压敏效应的低渗透油藏非线性流动特征

刘文超,姚 军,李爱芬,孙致学,黄朝琴

(中国石油大学(华东)石油工程学院,山东青岛 266555)

摘要:基于低渗透油藏非线性渗流速度函数导数的连续性,推导了实数域内低渗透油藏的非线性运动方程,确定了低渗透油藏视渗透率和视拟启动压力梯度的数学表达式,并论证了渗流速度函数导数连续与渗透率变化连续是相容的;建立了考虑压敏效应的低渗透油藏油井定产量生产时的非线性渗流数学模型;鉴于数学模型的强非线性,采用高效的有限差分 Douglas-Jones 预估校正法求得了其数值解,并与全隐式有限差分法所求数值解进行对比验证了解的正确性.结果分析表明:非线性运动方程和拟线性运动方程对应的瞬时无因次井底压力双对数曲线初期存在"拐点",拟线性运动方程对应双对数曲线的"拐点"更为突出;渗透率模数主要影响曲线后半段,其值越大,压力下降越剧烈;低渗透油藏非线性渗流存在动边界;拟线性流动动边界的传播速度比非线性流动的要慢.

关键词:低渗透油藏;压敏效应;有限差分 Douglas-Jones 预估校正法;非线性流动;动边界;试井

0 Introduction

At present, the reserves of low-permeability reservoirs are assuming an increasingly larger percentage of all reserves in many mature regions and countries. For example, in West Siberia of Russia, the reserves of low-permeability reservoirs and thin reservoirs account for in excess of 50% of the proven reserves. In China, at least 50% of the total oil and gas resources exist in the low-permeability reservoirs. Efficiently developing and utilizing low-permeability reservoirs is becoming an urgent task on hand for the world's energy supply[1-2]. The study on the models of the flow in low-permeability reservoirs can help to figure out some intrinsic laws, which can be incorporated into some petroleum engineering technologies such as numerical reservoir simulation and well testing, and is thus of great significance.

Recently, the study on the nonlinear/pseudo-linear flow in low-permeability reservoirs has become an important topic. It is well known that the tri-sectional model of the nonlinear kinematic equation[3-6] was put forward long time ago. It can precisely describe the seepage flow behavior in low-permeability reservoirs. However, due to the complexity of the relevant mathematical model, the pseudo-linear kinematic equation[7-11] is generally adopted to approximate the nonlinear one.

Current oilfield practices have proved that the threshold pressure gradient in the pseudo-linear kinematic equation is overestimated[12-13]. According to the pseudo-linear kinematic equation, no flow will happen further away from the oil well, because the pressure gradient is much smaller than the threshold pressure gradient. This is generally inconsistent with the actual situation in well production[12]. Besides, in low-permeability reservoirs the pore throats are very tiny, where the seepage resistance will be rather large; as a result, the pressure drop will be very sharp during the flowing process. The sharp decrease in formation pressure can deform the rock, which makes the stress sensitive effect[14-16] much more serious. In this paper, in consideration of the actual situations mentioned above in the development of low permeability reservoirs, a mathematical model of the nonlinear flow in low-permeability reservoirs with stress sensitive effect is built.

1 Deduction of the nonlinear kinematic equation

In low-permeability reservoirs pores and

throats are very tiny, and the interface area is very large, therefore the interaction between the rock and fluid is rather intense[3,17-18], and the micro scale effect is very serious. Many surface reactive materials such as asphaltum, clay, etc, adhere to the inner rock surface and form boundary layers[17-18], which can resist the fluid flow in the rock. Besides, the radius difference among pore throats in low-permeability reservoirs is very large, and the heterogeneity is very strong. When the driving pressure gradient is small, the fluid can't flow through tiny pore throats or the marginal areas of large pore throats, but through the center areas of large pore throats. The two factors make the permeability in low-permeability reservoirs not constant, but mutative[12-13]: with the increase of driving pressure gradient, the thickness of boundary layers becomes thinner and thinner, and more and more small throats and regions of large throats participate in the seepage flow; as a result, the permeability increases gradually until up to a maximum value.

The tri-sectional model[3,5] of the nonlinear kinematic equation can accurately depict the flow behavior in low-permeability reservoirs (see Fig. 1). It includes non-flow region OE, nonlinear flow region EF and pseudo-linear flow region FG; OE shows small pressure gradient can't drive the fluid flow; EF indicates the gradual increase of the permeability, where the relationship between the seepage velocity and pressure gradient is power law[3,6]; FG represents the pseudo-linear flow, where the permeability fully recovers and doesn't change any more. In order to be convenient for mathematical treatment, FG and its reverse extension line, whose arrival is at the point of intersection with x-coordinate, i. e. the pseudo-linear kinematic equation[7] is generally adopted to approximate the nonlinear one. The intercept is the pseudo threshold pressure gradient λ_B, MPa/m. The pressure gradient at point E is the threshold pressure gradient λ_C, MPa/m; the pressure gradient at point F is the critical pressure

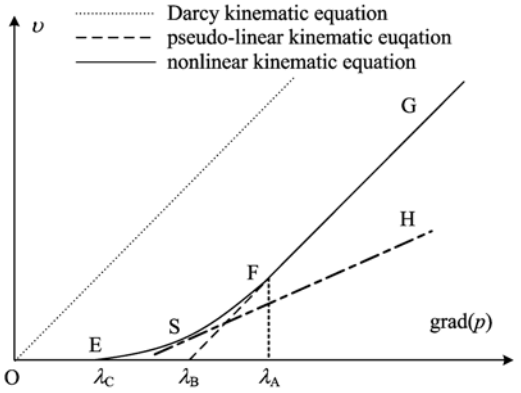

Fig. 1　The schematics of three different kinematic equations

gradient λ_A, MPa/m. the nonlinear kinematic equation can be expressed as follows[3,6]:

$$\upsilon=\begin{cases}0,\ 0<\dfrac{\mathrm{d}p}{\mathrm{d}r}\leqslant\lambda_C;\\ -C\dfrac{k}{\mu}\left(\dfrac{\mathrm{d}p}{\mathrm{d}r}-\lambda_C\right)^n,\ \lambda_C<\dfrac{\mathrm{d}p}{\mathrm{d}r}\leqslant\lambda_A;\\ -\dfrac{k}{\mu}\left(\dfrac{\mathrm{d}p}{\mathrm{d}r}-\lambda_B\right),\ \dfrac{\mathrm{d}p}{\mathrm{d}r}>\lambda_A.\end{cases}\quad(1)$$

Here $C/(\mathrm{MPa}\cdot\mathrm{m}^{-1})^{1-n}$ is a constant parameter to be determined; $k/\mu\mathrm{m}^2$ is the rock permeability fully recovering; $\mu/(\mathrm{mPa}\cdot\mathrm{s})$ is the fluid viscosity; p/MPa is the formation pressure; r/m is the radial distance; $\upsilon/(\mathrm{m}\cdot\mathrm{d}^{-1})$ is the seepage velocity; n/f is the power exponent.

From nonlinear fitting curves[3,19] of core experiments for low-permeability reservoirs, it can be seen that the curve for the nonlinear kinematic equation (see Fig. 1) is very smooth. A basic assumption was made that the nonlinear seepage velocity function with respect to the pressure gradient has continuous first-order derivative. Then the mathematical formula of the nonlinear kinematic equation can be further deduced with three experiment-determined parameters λ_A, λ_B and λ_C.

According to the continuity of the first order derivative at point F, we obtain

$$-\frac{k}{\mu}Cn(\lambda_A-\lambda_C)^{n-1}=-\frac{k}{\mu}.\quad(2)$$

Then C can be quantified as follows:

$$C=1/n/(\lambda_A-\lambda_C)^{n-1}.\quad(3)$$

Besides, according to the continuity of the seepage

velocity function at point F, we can obtain

$$n=(\lambda_A-\lambda_C)/(\lambda_A-\lambda_B),\ n>1. \tag{4}$$

In the model computation, the pressure gradient may be minus. The tri-sectional model of nonlinear kinematic equation in low-permeability reservoirs can be extended in the real number field by origin of symmetry, as follows:

$$\upsilon\left(\frac{\mathrm{d}p}{\mathrm{d}r}\right)=\begin{cases}0, & \left|\dfrac{\mathrm{d}p}{\mathrm{d}r}\right|\leqslant\lambda_C;\\ -\left(\dfrac{\mathrm{d}p}{\mathrm{d}r}\Big/\left|\dfrac{\mathrm{d}p}{\mathrm{d}r}\right|\right)\cdot\dfrac{k}{\mu}\cdot\dfrac{1}{n\cdot(\lambda_A-\lambda_C)^{n-1}}\left(\left|\dfrac{\mathrm{d}p}{\mathrm{d}r}\right|-\lambda_C\right)^n, & \lambda_C<\left|\dfrac{\mathrm{d}p}{\mathrm{d}r}\right|\leqslant\lambda_A;\\ -\left(\dfrac{\mathrm{d}p}{\mathrm{d}r}\Big/\left|\dfrac{\mathrm{d}p}{\mathrm{d}r}\right|\right)\cdot\dfrac{k}{\mu}\cdot\left(\left|\dfrac{\mathrm{d}p}{\mathrm{d}r}\right|-\lambda_B\right), & \left|\dfrac{\mathrm{d}p}{\mathrm{d}r}\right|>\lambda_A.\end{cases} \tag{5}$$

Experimental data i. e. velocity & pressure gradient[19] nonlinear fitting can easily verify the correctness of Eq. (4). From Eq. (4) it can also be seen that, if $\lambda_C=\lambda_B$, then $n=1.0$, and Eq. (5) turns to the pseudo-linear kinematic equation for the fluid flow in low permeability reservoirs; further, if $\lambda_C=\lambda_B=0$, Eq. (5) turns to the Darcy's law. Thus, Eq. (5) covers Darcy's law and pseudo-linear kinematic equation.

In Eq. (5), the first-order derivative of the seepage velocity with respect to the pressure gradient is continuous. So mark point S $(\left.\dfrac{\mathrm{d}p}{\mathrm{d}r}\right|_S,\upsilon_S)$ arbitrarily in the curve corresponding to the nonlinear kinematic equation and plot its tangent SH (see Fig. 1). At the small interval of point S, the seepage flow can be considered as pseudo-linear flow, which can be represented by the line SH, and its kinematic equation is as follows:

$$\upsilon=\upsilon'\left(\left.\frac{\mathrm{d}p}{\mathrm{d}r}\right|_S\right)\cdot\left(\frac{\mathrm{d}p}{\mathrm{d}r}-\left.\frac{\mathrm{d}p}{\mathrm{d}r}\right|_S+\upsilon\left(\left.\frac{\mathrm{d}p}{\mathrm{d}r}\right|_S\right)/\upsilon'\left(\left.\frac{\mathrm{d}p}{\mathrm{d}r}\right|_S\right)\right), \tag{6}$$

where $\upsilon'/(\mathrm{m^2\cdot d^{-1}\cdot MPa^{-1}})$ is the derivative of the seepage velocity function with respect to the pressure gradient and can be expressed as follows:

$$\upsilon'\left(\frac{\mathrm{d}p}{\mathrm{d}r}\right)=\begin{cases}0, & \left|\dfrac{\mathrm{d}p}{\mathrm{d}r}\right|\leqslant\lambda_C;\\ -\dfrac{k}{\mu(\lambda_A-\lambda_C)^{n-1}}\left(\left|\dfrac{\mathrm{d}p}{\mathrm{d}r}\right|-\lambda_C\right)^{n-1}, & \lambda_C<\left|\dfrac{\mathrm{d}p}{\mathrm{d}r}\right|\leqslant\lambda_A;\\ -\dfrac{k}{\mu}, & \left|\dfrac{\mathrm{d}p}{\mathrm{d}r}\right|>\lambda_A.\end{cases} \tag{7}$$

In comparison of Eq. (6) with the pseudo-linear kinematic equation[7], the apparent permeability $k_b/\mu\mathrm{m^2}$, and the apparent pseudo threshold pressure gradient $G_b/(\mathrm{MPa\cdot m^{-1}})$, can be respectively expressed as follows:

$$k_b=-\upsilon'\cdot\mu, \tag{8}$$

$$G_b=\frac{\mathrm{d}p}{\mathrm{d}r}-\frac{\upsilon}{\upsilon'}. \tag{9}$$

The first-order derivative of the seepage velocity function i. e. Eq. (7) is continuous, and then from Eqs. (8)～(9) the apparent permeability and the apparent pseudo threshold pressure gradient with respect to the pressure gradient are both continuous, which accords with the objective principle of gradual permeability change[3,17,20] in low-permeability reservoirs. Contrariwise, from Eqs. (7)～(8) the continuous permeability change in low-permeability reservoirs can also guarantee the continuity of the first-order derivative of the nonlinear seepage velocity function. Therefore, the continuous first-order derivative of the nonlinear seepage velocity function is consistent with the continuous permeability change, and thus the basic assumption of continuous first-order derivative of the nonlinear seepage velocity function is reasonable.

2 Mathematical modeling

The problem considered here involves production of oil from a fully penetrating well at the center of a cylindrical low-permeability reservoir; some assumptions are as follows:

① The reservoir is homogenous, isotropic and isothermal with closed ceiling and bottom

boundaries.

② Single-phase, horizontal and radial flow without considering gravity effect.

③ Eq. (5) is applied as the kinematic equation.

④ The fluid and rock are slightly compressible.

The fluid density[21] can be expressed as follows:

$$\rho(p) = \rho_i[1 + C_f(p - p_i)], \tag{10}$$

where p_i/MPa is the initial formation pressure; ρ_i/(kg · m^{-3}) is the initial fluid density; ρ/(kg · m^{-3}) is the fluid density; C_f/MPa^{-1} is the fluid compression coefficient.

The rock porosity[21] can be expressed as follows:

$$\varphi(p) = \varphi_i[1 + C_\varphi(p - p_i)], \tag{11}$$

where φ/f is the porosity; φ_i/f is the initial porosity; C_φ/MPa^{-1} is the porosity compression coefficient.

The permeability modulus, γ/MPa^{-1}, is similar to the compressibility coefficient, and can be defined by the following equation[14-16]:

$$\gamma = \frac{1}{k}\frac{\mathrm{d}k}{\mathrm{d}p}. \tag{12}$$

Coefficient γ plays an important role in the stress sensitive effect towards the rock permeability. It is the measurement of the dependence of the permeability on the formation pressure. For practical use, γ can be assumed to be constant. So the permeability of deformed rock in low-permeability reservoirs can be expressed as follows:

$$k = k_i e^{-\gamma(p_i - p)}, \tag{13}$$

where k_i/μm^2 is the rock permeability at the initial pressure.

The continuous equation for the radial flow[21] is as follows:

$$-\frac{1}{r}\frac{\partial}{\partial r}(r\rho v) = \frac{\partial(\rho\varphi)}{\partial t}. \tag{14}$$

Substituting state equations Eqs. (10)～(13) and nonlinear kinematic equation Eq. (5) into the continuous equation above, we obtain

$$-\frac{e^{-\gamma(p_i - p)}}{r}\left(v\left(\frac{\partial p}{\partial r}\right) + r\frac{\partial^2 p}{\partial r^2}v'\left(\frac{\partial p}{\partial r}\right) + \gamma\frac{\partial p}{\partial r}rv\right) = \varphi_i C_t\frac{\partial p}{\partial t}, \tag{15}$$

where C_t/MPa^{-1} is the total compression coefficient; t/h is the time.

The initial condition is as follows:

$$p(r,t)\,|_{t=0} = p_i. \tag{16}$$

Because near the wellbore the pressure gradient is much larger than the critical pressure gradient λ_A, the inner boundary condition of constant well production can be written as follows:

$$\frac{2\pi khr_w}{\mu B}e^{-\gamma(p_i - p)}\left(\frac{\mathrm{d}p}{\mathrm{d}r} - \lambda_B\right)\Big|_{r=r_w} = q_0, \tag{17}$$

where r_w/m is the radius of the wellbore; q_0/(m^3 · d^{-1}) is the well production rate; B/(m^3 · m^{-3}) is the volume factor of the crude oil; h/m is the thickness of the reservoir.

The outer boundary condition of constant pressure is as follows:

$$p(r,t)\,|_{r=r_e} = p_i, \tag{18}$$

where r_e/m is the radius of the outer boundary.

Nondimensionalizing Eqs. (15) ～ (18), we have

$$\frac{e^{-\gamma_D P_D}}{r_D}\left[v_D\left(\frac{\partial P_D}{\partial r_D}\right) - r_D \cdot v_D'\left(\frac{\partial P_D}{\partial r_D}\right)\cdot\frac{\partial^2 P_D}{\partial r_D^2} - \gamma_D \cdot \frac{\partial P_D}{\partial r_D}\cdot r_D \cdot v_D\left(\frac{\partial P_D}{\partial r_D}\right)\right] = \frac{\partial P_D}{\partial t_D}, \tag{19}$$

$$P_D\,|_{t_D=0} = 0, \tag{20}$$

$$e^{-\gamma_D P_D}\left(\frac{\partial P_D}{\partial r_D}\Big|_{r_D=1} + G_B\right) = -1, \tag{21}$$

$$P_D\,|_{r_D=r_{eD}} = 0. \tag{22}$$

Eqs. (19)～(22) construct the dimensionless mathematical model of the nonlinear flow in low-permeability reservoirs with stress sensitive effect.

$$r_D = \frac{r}{r_w},\ t_D = \frac{3.6k}{\varphi_i C_t \mu r_w^2}t,$$

$$r_{eD} = \frac{r_e}{r_w},\ G_A = \frac{khr_w\lambda_A}{1.842\times10^{-3}q_0\mu B},$$

$$P_D(r_D,t_D) = \frac{kh}{1.842\times10^{-3}q_0\mu B}[p_i - p(r,t)],$$

$$G_B = \frac{khr_w\lambda_B}{1.842\times10^{-3}q_0\mu B},$$

$$G_C = \frac{khr_w\lambda_C}{1.842\times10^{-3}q_0\mu B},$$

$$\gamma_D = \frac{1.842\times10^{-3} q_0 \mu B \gamma}{kh},$$

where r_D is the dimensionless radius; r_{eD} is the dimensionless radius of the outer boundary; t_D is the dimensionless time; P_D is the dimensionless formation pressure; G_A is the dimensionless critical pressure gradient; G_B is the dimensionless pseudo-linear pressure gradient; G_C is the dimensionless threshold pressure gradient; υ_D is the dimensionless seepage velocity; υ'_D is the dimensionless derivative of the seepage velocity; γ_D is the dimensionless permeability modulus.

3 Numerical solution of the mathematical model

First, the authors perform the logarithmic transformation $x = \ln(r_D)$, Eqs. (19) ~ (22) become

$$\upsilon_D\left(\frac{1}{e^x}\cdot\frac{\partial P_D}{\partial x}\right) - e^x\cdot\upsilon'_D\left(\frac{1}{e^x}\cdot\frac{\partial P_D}{\partial x}\right)\cdot\left(-\frac{1}{e^{2x}}\cdot\frac{\partial P_D}{\partial x}+\frac{1}{e^{2x}}\cdot\frac{\partial^2 P_D}{\partial x^2}\right) - \gamma_D\cdot\frac{\partial P_D}{\partial x}\cdot\upsilon_D\left(\frac{1}{e^x}\cdot\frac{\partial P_D}{\partial x}\right) = e^{x+\gamma_D P_D}\cdot\frac{\partial P_D}{\partial t_D}, \quad (23)$$

$$P_D\big|_{t_D=0} = 0, \quad (24)$$

$$e^{-\gamma_D P_D}\left(\frac{\partial P_D}{\partial x}\Big|_{x=0} + G_B\right) = -1, \quad (25)$$

$$P_D\big|_{x=\ln(r_{eD})} = 0. \quad (26)$$

Douglas-Jones predictor-corrector method[22-23] is an implicit finite difference method based on implicit linearization for numerical solution of nonlinear parabolic PDEs. It only requires two iterations per time step. Babajimopoulos[24-25] obtained the accuracy-verified numerical solutions of Richards equations for unsaturated flow problems in soils by Douglas-Jones predictor-corrector method. The strong nonlinear PDE for the flow in low-permeability reservoirs with stress sensitive effect i. e. Eq. (23) has the similar form with Richards equations involving piecewise functions and strong nonlinear terms. Douglas-Jones predictor-corrector method can make them explicit in the difference equations and it is unnecessary to iterate them, which can largely improve computational efficiency and numerical stability.

The Douglas-Jones predictor scheme for Eq. (23) (time step from j to $j+1/2$) is as follows[22-23]:

$$\begin{aligned} &e^{i\Delta x}\cdot\upsilon_D\left(\frac{1}{e^{i\Delta x}}\cdot(P^j_{Di+1}-P^j_{Di-1})/2/\Delta x\right) - \\ &\upsilon'_D\left(\frac{1}{e^{i\Delta x}}\cdot(P^j_{Di+1}-P^j_{Di-1})/2/\Delta x\right)\cdot \\ &\Big(-(P^j_{Di+1}-P^j_{Di-1})/2/\Delta x + \\ &(P^{j+\frac12}_{Di+1}-2P^{j+\frac12}_{Di}+P^{j+\frac12}_{Di-1})/2/\Delta x\Big) - \\ &\gamma_D\cdot e^{i\Delta x}\cdot(P^j_{Di+1}-P^j_{Di-1})/2/\Delta x\cdot \\ &\upsilon_D\left(\frac{1}{e^{i\Delta x}}\cdot(P^j_{Di+1}-P^j_{Di-1})/2/\Delta x\right) = \\ &2\cdot e^{2i\Delta x+\gamma_D P^j_{Di}}\cdot(P^{j+\frac12}_{Di}-P^j_{Di})/\Delta t, \end{aligned} \quad (27)$$

where i, j is the space index and the time index, respectively.

The predictor scheme for the inner boundary condition is

$$P^{j+\frac12}_{D-1} = P^{j+\frac12}_{D1} + 2\Delta x\cdot(e^{\gamma_D P^j_{D0}} + G_B). \quad (28)$$

The Douglas-Jones corrector scheme (time step from $j+1/2$ to $j+1$) for Eq. (23) is as follows[22-23]:

$$\begin{aligned} &e^{i\Delta x}\cdot\upsilon_D\left(\frac{1}{e^{i\Delta x}}\cdot(P^{j+\frac12}_{Di+1}-P^{j+\frac12}_{Di-1})/2/\Delta x\right) - \\ &\upsilon'_D\left(\frac{1}{e^{i\Delta x}}\cdot(P^{j+\frac12}_{Di+1}-P^{j+\frac12}_{Di-1})/2/\Delta x\right)\cdot \\ &\Big((P^{j+\frac12}_{Di-1}-P^{j+\frac12}_{Di+1})/2/\Delta x + \\ &\frac{1}{2(\Delta x)^2}((P^{j+1}_{Di+1}-2P^{j+1}_{Di}+P^{j+1}_{Di-1}) + \\ &(P^j_{Di+1}-2P^j_{Di}+P^j_{Di-1}))\Big) - \\ &\gamma_D\cdot e^{i\Delta x}\cdot(P^{j+\frac12}_{Di+1}-P^{j+\frac12}_{Di-1})/2/\Delta x\cdot \\ &\upsilon_D\left(\frac{1}{e^{i\Delta x}}\cdot(P^{j+\frac12}_{Di+1}-P^{j+\frac12}_{Di-1})/2/\Delta x\right) = \\ &e^{2i\Delta x+\gamma_D P^{j+\frac12}_{Di}}\ \frac{P^{j+1}_{Di}-P^j_{Di}}{\Delta t}. \end{aligned} \quad (29)$$

The corrector scheme for the inner boundary condition is

$$P^{j+1}_{D-1} = P^{j+1}_{D1} + 2\Delta x\cdot(e^{\gamma_D P^{j+\frac12}_{D0}} + G_B). \quad (30)$$

Scheme of the initial boundary condition:

$$P^0_{Di} = 0,\ i = 0,\cdots,M. \quad (31)$$

Scheme of the outer boundary condition:

$$P_{\mathrm{DN}}^{j}=0,\ j=0,\frac{1}{2},1,\frac{3}{2},\cdots,N. \tag{32}$$

Numerical solution with Douglas-Jones predictor-corrector method has two procedures. First, increasing half time step, the predicting pressures at every space grids when time step $j+1/2$ needs to be solved. From Eqs. (27)～(28) and Eqs. (31)～(32), it can be seen that the difference equations are tri-diagonal and linear, which can be solved by Thomas algorithm[26]. Second, increasing half time step once again, the pressures when time step $j+1$ can be corrected and obtained by Eqs. (29)～(32). For the corrector procedure, the difference equations are also tri-diagonal and linear, and can be solved by Thomas algorithm. The accuracy of Douglas-Jones predictor-corrector method is second-order[24-25].

In order to verify the accuracy of the numerical solution obtained by the Douglas-Jones predictor-corrector method, the fully implicit finite difference method[26] is also adopted. The fixed-point iteration scheme for the resulting nonlinear finite difference equations is as follows, where for every iteration a group of tri-diagonal and linear equations need to be solved by Thomas algorithm[26]:

$$\begin{aligned}&\mathrm{e}^{\mathrm{i}\Delta x}\cdot\upsilon_{\mathrm{D}}\left(\frac{1}{\mathrm{e}^{\mathrm{i}\Delta x}}\cdot(P_{\mathrm{D}i+1}^{j+1(m)}-P_{\mathrm{D}i-1}^{j+1(m)})/2/\Delta x\right)-\\&\upsilon_{\mathrm{D}}'\left(\frac{1}{\mathrm{e}^{\mathrm{i}\Delta x}}\cdot(P_{\mathrm{D}i+1}^{j+1(m)}-P_{\mathrm{D}i-1}^{j+1(m)})/2/\Delta x\right)\cdot\\&(-(P_{\mathrm{D}i+1}^{j+1(m+1)}-P_{\mathrm{D}i-1}^{j+1(m+1)})/2/\Delta x+\\&(P_{\mathrm{D}i+1}^{j+1(m+1)}-2P_{\mathrm{D}i}^{j+1(m+1)}+P_{\mathrm{D}i-1}^{j+1(m+1)})/2/\Delta x)-\\&\gamma_{\mathrm{D}}\cdot\mathrm{e}^{\mathrm{i}\Delta x}\cdot(P_{\mathrm{D}i+1}^{j+1(m+1)}-P_{\mathrm{D}i-1}^{j+1(m+1)})/2/\Delta x\cdot\\&\upsilon_{\mathrm{D}}\left(\frac{1}{\mathrm{e}^{\mathrm{i}\Delta x}}\cdot(P_{\mathrm{D}i+1}^{j+1(m)}-P_{\mathrm{D}i-1}^{j+1(m)})/2/\Delta x\right)=\\&2\cdot\mathrm{e}^{2\mathrm{i}\Delta x+\gamma_{\mathrm{D}}P_{\mathrm{D}i}^{j}}\cdot(P_{\mathrm{D}i}^{j+1(m+1)}-P_{\mathrm{D}i}^{j})/\Delta t,\end{aligned} \tag{33}$$

where m is the iteration times.

4 Result analysis

4.1 Accuracy verification

Fig. 2 is the comparison figure of dimensionless transient wellbore pressures computed by Douglas-Jones predictor-corrector method and fully implicit finite difference method. From Fig. 2, it can be seen that the log-log curves of dimensionless transient wellbore pressures computed by the two methods have excellent agreement with each other, and so the accuracy of the numerical solution by Douglas-Jones predictor-corrector method can be verified.

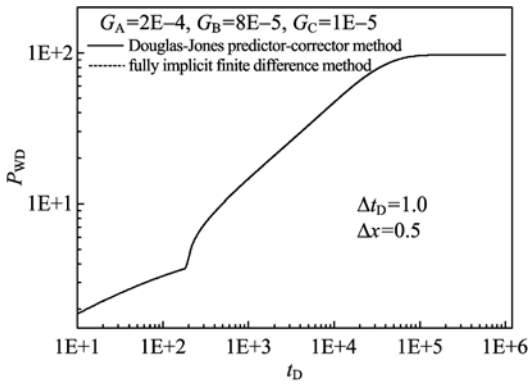

Fig. 2　Comparison of dimensionless transient wellbore pressures computed by the two methods

Besides, from Fig. 2 it can also be shown that log-log curves of dimensionless transient wellbore pressures have inflexions at the initial period. Before the inflexions, the curves are straight, and the dimensionless wellbore pressures increase slowly. After the inflexions, the pressures go up quickly, reaching eventually a stable state when the pressures don't change any more.

4.2　Influence of stress sensitive effect

Fig. 3 is the comparison figure of dimensionless transient wellbore pressures under

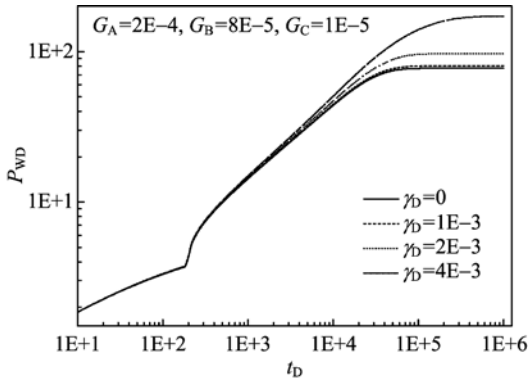

Fig. 3　The effect of dimensionless permeability modulus on dimensionless transient wellbore pressure

different values of dimensionless permeability modulus. From Fig. 3, it can be seen that the dimensionless permeability modulus has the main effect on the second half of these curves. The bigger its value, the faster the dimensionless wellbore pressures ascending, and the later the arrival time of the stable state. The permeability modulus indicates the degree of stress sensitive effect. The bigger its value, the more serious the stress sensitive effect, the more the energy consumption for the flow in the formation, and the sharper the pressure drop.

4.3 Comparison of dimensionless transient wellbore pressures corresponding to three different kinematic equations

Fig. 4 is the comparison figure of dimensionless transient wellbore pressures corresponding to three different kinematic equations. From Fig. 4, it can be seen that the influence of different kinematic equations for low-permeability reservoirs on the dimensionless transient wellbore pressure mainly focuses on the initial period of well production. The curve corresponding to the Darcy kinematic equation is very smooth and doesn't have inflexions; but the curves corresponding to the nonlinear and pseudo-linear kinematic equations both have inflexions, and the inflexion for the pseudo-linear one is more obvious; but at last these curves converge together. Because the nonlinear and pseudo-linear kinematic equations are both sectional functions, and so different flow regions of pressure gradient obey different rules, which results in the occurrence of inflexions on these curves; especially, for the pseudo-linear kinematic equation, larger threshold pressure gradient makes its inflexion on curves more obvious.

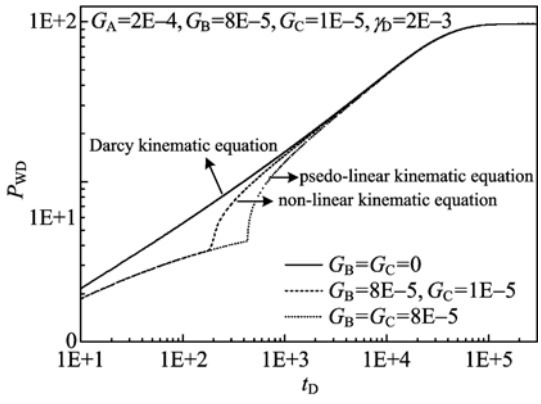

Fig. 4 Comparison of dimensionless transient wellbore pressure corresponding to different kinematic equations

4.4 Existence of moving boundary

From Tab. 1, it can be seen that when t_D = 100, the dimensionless pressures corresponding to three different kinematic equations all decrease gradually from the inner boundary to the outer boundary; on every spatial grid, except for the one at the outer boundary with constant pressure, the dimensionless pressure of Darcy flow are all bigger than zero, and so to the entire reservoir can the pressure wave propagate. For the nonlinear kinematic equation and the pseudo-linear kinematic equation, dimensionless pressures are zero outside certain spatial grids, where the resulting pressure gradients are zero and then the fluid can't flow. Fig. 5 displays the change of dimensionless pressure distribution with the increase of dimensionless time. From Fig. 5, it can also be seen with the increase of the dimensionless time, the pressure wave of the nonlinear flow expands outside gradually. Therefore, the existence of the moving boundary for the nonlinear flow in low-permeability reservoirs is validated here. From Tab. 1, it can also be concluded that the moving boundary of the pseudo-linear flow propagates more slowly than that of the nonlinear flow.

Tab. 1 Data of pressure distributions corresponding to three different kinematic equations, when t_D =100

x	Darcy	nonlinear	pseudo-linear
1.0	4.5	1.8	1.8
3.4	0.1	0.03	0.008
3.5	0.005	0.01	0
3.6	0.025	0.001	0
4.0	7.4E−5	0	0
4.9	1.2E−18	0	0
5.2	9.6E−26	0	0
$\ln(r_{eD})$	0	0	0

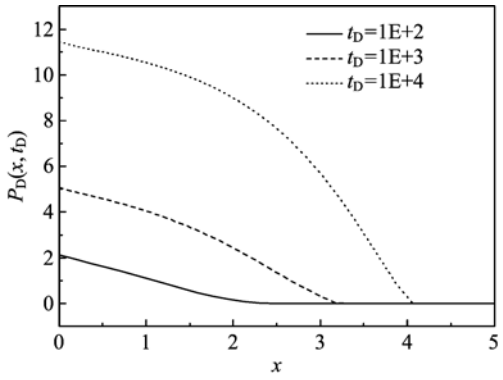

Fig. 5　The change of dimensionless pressure distribution with the increase of dimensionless time

5　Conclusion

(Ⅰ) Based on the continuity of the first order derivative of the seepage velocity function in low-permeability reservoirs, the nonlinear kinematic equation for the low-permeability reservoirs was deduced. It's very convenient for the reservoir modeling and computation.

(Ⅱ) Based on the nonlinear kinematic equation, the mathematical model of the nonlinear flow in low-permeability reservoirs with stress sensitive effect was constructed. It is much more practical than previous models such as models of the pseudo-linear flow or models with no consideration of stress-sensitive effect in low-permeability reservoirs. The implicit Douglas-Jones predictor-corrector method was adopted to obtain its numerical solution with fast computational velocity, good numerical stability and second-order accuracy. The solution was also verified by the comparison with the numerical solution obtained by the fully implicit finite difference method. The research on the constructed model can support theoretical foundation for numerical well testing in low-permeability reservoirs.

(Ⅲ) Result analysis shows: log-log curves of dimensionless transient wellbore pressure for the nonlinear flow in low-permeability reservoirs have inflexions at the initial period; the inflexion for the pseudo-linear flow is more obvious; the dimensionless permeability modulus has a major effect on the second half of these curves, the bigger its value, the sharper the wellbore pressure drop; there exists a moving boundary for the nonlinear flow in low-permeability reservoirs.

References

[1] Luo Pingya, Meng Yingfeng, Shu Shihong, et al. Some problems in the exploration and exploitation low permeability of oil and gas resources in China[C]// SPE 50923, Beijing, China, 1998.

[2] You Yuan, Yue Xiangan, Li Mingyi, et al. Physical simulation of fluid flow and production performance in extra-low permeability porous medium[J]. Petroleum Science, 2009, 36(4): 415-420.

[3] Huang Yanzhang. Mechanism of the Flow in Low Permeability Reservoir [M]. Beijing: Petroleum Industry Press, 1998.

[4] Li Aifen, Liu Min, Zhang Shaohui, et al. Experimental study on the percolation characteristics of extra low-permeability reservoir[J]. Journal of Xi'an Shiyou University (Natural Science Edition), 2008, 23(2): 36-39.

[5] E Jian, Chen Gang, Sun Airong. One-dimensional consolidation of saturated cohesive soil considering non-Darcy flows [J]. Chinese Journal of Geotechnical Engineering, 2009, 31(7): 1 115-1 119.

[6] Hansbo S. Aspects of vertical drain design: Darcian or non-Darcian flow[J]. Geotechnique, 1997, 47(5): 983-992.

[7] Prada A, Civan F. Modification of Darcy's law for the threshold pressure gradient[J]. Journal of Petroleum Science and Engineering, 1999, 22: 237-240.

[8] Huang Feng, Lu Detang. Computation of non-Darcy flow with hybrid grids [J]. Chinese Journal of Computational Physics, 2007, 24(4): 419-425.

[9] Yin D Y, Pu H. Numerical simulation study on surfactant flooding for low permeability oilfield in the condition of threshold pressure [J]. Journal of Hydrodynamics, Ser B, 2008, 20(4): 492-498.

[10] Song H Q, Zhu W Y, Wang M, et al. A study of effective deloyment in ultra-low-permeability reservoirs with non-Darcy flow [J]. Petroleum Science and Technology, 2010, 28(16): 1 700-1 711.

[11] Yao Yuedong, Ge Jiali. Characteristics of non-Darcy flow in low-permeability reservoirs [J]. Petroleum Science, 2011, 8(1): 55-62.

[12] Lei Qun, Xiong Wei, Yun Jiangru, et al. Behavior of flow through low-permeability reservoirs[C]// SPE

113144. Rome, Italy, 2008.

[13] Xiong Wei, Lei Qun, Gao Shusheng, et al. Pseudo threshold pressure gradient to flow for low-permeability reservoirs[J]. Petroleum Exploration and Development, 2009, 36(2): 232-236.

[14] Ruan Min, Wang Liangang. The development of the low permeability reservoir and stress-sensitive effect [J]. Acta Petrolei Sinica, 2002, 23(3): 46-49.

[15] Rosalind A. Impact of stress sensitive permeability on production data analysis[C]// SPE 114166, Colorado, USA, 2008.

[16] Torsten F, Hans-Dieter V. Analytical solutions for the radial flow equation with constant-rate and constant-pressure boundary conditions in reservoirs with pressure-sensitive permeability [C]// SPE 122768, Colorado, USA, 2009.

[17] Wang Fei, Yue Xiangan, Xu Shaoliang, et al. Influence of wettability on flow characteristics of water through microtubes and cores[J]. Chinese Sci Bull, 2009, 54(7): 972-977.

[18] Rene R M, Wayner P C. Aqueous wetting films on fused quartz [J]. J Colloid Interface Sci, 1999, 214(2): 156-169.

[19] Yang R F. The foundational theory of nonlinear flow in porous media and numerical simulation in low permeability reservoirs[D]. Qingdao: China University of Petroleum, 2010.

[20] Yao Jun, Liu Shun. Well test interpretation model based on mutative permeability effects for low-permeability reservoir[J]. Acta Petrolei Sinica, 2009, 30(3): 430-433.

[21] Zhang Jianguo, Lei Guanglun, Zhang Yanyu. Mechanics of Porous Media Flow in Hydrocarbon Reservoir[M]. Shandong Dongying: China University of Petroleum Press, 2006.

[22] Ma Xiaodan, Tong Dengke, Ma Hua-wei. Non-Darcy flow analysis of fluid in deformed fractal reservoir with double porosity[J]. Chinese Journal of Computational Physics, 2007, 24(2): 198-202.

[23] Islam M N, Azaiez J. Nonlinear simulation of thermo-viscous fingering in nonisothermal miscible displacements in porous medium [C]// SPE103243, San Antonio, USA, 2006.

[24] Babajimopoulos C. A Douglas-Jones predictor-corrector program for simulating one-dimensional unsaturated flow in soil [J]. Ground Water, 1991, 29 (2): 267-269.

[25] Babajimopoulos C. Revisiting the Douglas-Jones method for modeling unsaturated flow in a cultivated soil[J]. Environ Model & Softw, 2002, 15 (3): 303-312.

[26] Burden R L, Faires J D. Numerical Analysis [M]. 8th ed. Belmont, CA: Thomason Higher Education, 2005.